



Article

# Silencing *GmBIR1* in Soybean Results in Activated Defense Responses

Dan-Dan Liu <sup>1,†</sup>, Hu-Jiao Lan <sup>1,†</sup>, Hashimi Said Masoud <sup>1</sup> , Mei-Yan Ye <sup>1</sup>, Xian-Yong Dai <sup>1</sup>, Chen-Li Zhong <sup>1</sup>, Sheng-Nan Tian <sup>1</sup> and Jian-Zhong Liu <sup>1,2,\*</sup>

<sup>1</sup> Institute of Plant Genetics and Developmental Biology, College of Chemistry and Life Sciences, Zhejiang Normal University, Jinhua 321004, China; dandanliu@163.com (D.-D.L.); 18659351751@163.com (H.-J.L.); s.masoud.hashimi@gmail.com (H.S.M.); a19557861320@163.com (M.-Y.Y.); q1178261391@163.com (X.-Y.D.); 18170141671@163.com (C.-L.Z.); xiaotian12260606@163.com (S.-N.T.)

<sup>2</sup> Zhejiang Provincial Key Laboratory of Biotechnology on Specialty Economic Plants, Zhejiang Normal University, Jinhua 321004, China

\* Correspondence: jzliu@zjnu.cn; Tel.: +86-579-8228-8053; Fax: +86-579-8228-2269

† These authors contributed to this work equally.

**Abstract:** Receptor-like kinases (RLKs) are a large group of pattern recognition receptors (PRRs) and play a critical role in recognizing pathogens, transducing defense signals, and mediating the activation of immune defense responses. Although extensively studied in the model plant *Arabidopsis*, studies of RLKs in crops, including soybean, are limited. When a *BAK1-interacting receptor-like kinase (BIR1)* homolog (referred to as *GmBIR1* hereafter) was silenced by the BPMV (*Bean pod mottle virus*)-induced gene silencing (BPMV-VIGS), it resulted in phenotypes that were reminiscent of constitutively activated defense responses, including a significantly stunted stature with observable cell death on the leaves of the silenced plants. In addition, both SA and H<sub>2</sub>O<sub>2</sub> were over-accumulated in the leaves of the *GmBIR1*-silenced plants. Consistent with this autoimmune phenotype, *GmBIR1*-silenced plants exhibited significantly enhanced resistance to both *Pseudomonas syringae* *pv. glycinea* (*Psg*) and *Soybean mosaic virus* (*SMV*), two different types of pathogens, compared to the vector control plants. Together, our results indicated that *GmBIR1* is a negative regulator of immunity in soybean and the function of BIR1 homologs is conserved in different plant species.

**Keywords:** *Glycine max*; virus-induced gene silencing (VIGS); receptor-like kinases; immune responses; BIR1; salicylic acid



**Citation:** Liu, D.-D.; Lan, H.-J.; Masoud, H.S.; Ye, M.-Y.; Dai, X.-Y.; Zhong, C.-L.; Tian, S.-N.; Liu, J.-Z. Silencing *GmBIR1* in Soybean Results in Activated Defense Responses. *Int. J. Mol. Sci.* **2022**, *23*, 7450. <https://doi.org/10.3390/ijms23137450>

Academic Editors: Andrés J. Cortés and Hai Du

Received: 7 June 2022

Accepted: 30 June 2022

Published: 5 July 2022

**Publisher's Note:** MDPI stays neutral with regard to jurisdictional claims in published maps and institutional affiliations.



**Copyright:** © 2022 by the authors. Licensee MDPI, Basel, Switzerland. This article is an open access article distributed under the terms and conditions of the Creative Commons Attribution (CC BY) license (<https://creativecommons.org/licenses/by/4.0/>).

## 1. Introduction

Pathogen-associated molecular patterns (PAMPs) are conserved microbial components that can be perceived by plasma membrane-localized pattern recognition receptors (PRRs) and trigger immunity [1]. The PRRs constitute the largest gene family (>600 genes) in *Arabidopsis* [2]. The PRRs include two types of protein families: the receptor-like kinases (RLKs) and receptor-like proteins (RLPs). While a typical RLK contains an extracellular leucine-rich repeat (LRR) domain, a transmembrane domain (TM), and a cytoplasmic kinase domain, an RLP contains only LRR and TM domains but lacks a cytoplasmic kinase domain. The LRR domain is responsible for perception of PAMPs or ligands, and the cytoplasmic kinase domain is involved in intracellular signal transduction [3]. The lack of a kinase domain in a RLP suggests that an RLP needs to pair with RLKs or another cytoplasmic kinase to transduce signals [3].

Some RLKs have been reported to sense PAMPs either from bacteria or fungi and transduce defense signals [4]. The best studied examples are FLAGELLIN SENSING2 (FLS2) and EF-TU RECEPTOR (EFR). FLS2 recognizes the 22 amino acid peptide flg22 from bacterial flagellin, while EFR recognizes an 18 amino acid peptide, elf18, derived from bacterial translation elongation factor EF-TU [5,6]. BAK1 was originally identified as a

BIR1 interacting protein, and it forms a protein complex with BIR1 during perception of Brassinosteroids (BRs) [7,8]. It is now clear that BAK1 serves as a common co-receptor for different RLKs or even RLPs that sense ligands ranging from BRs to PAMPs. Upon ligand or PAMP recognition, BAK1 is recruited to form a complex with RLKs such as FLS2, EFR and CERK1 [9–11]. The ligand-induced RLKs–BAK1 complex formation initiates dynamic trans-phosphorylation between the receptor, co-receptor, and receptor-like cytoplasmic kinases (RLCKs) such as BOTRYTIS-INDUCED KINASE1 (BIK1) [12,13], thus leading to the activation of downstream signaling.

Using isotope-coded affinity tag reagents and mass spectrometry, Gao et al. [14] identified BAK1 as BIR1-interacting protein on the plasma membrane (PM), which was subsequently confirmed by BiFC and Co-IP assays [14]. BIR1 belongs to the LRRX group of RLKs, with 620 amino acids and 5 LRRs. Compared to RLKs such as FLS2 or BAK1, BIR1 is a smaller protein with a significantly reduced number of LRR repeats [14]. Loss of function of *BIR1* in Arabidopsis leads to extensive cell death, induction of *PR* genes, enhanced accumulation of SA and H<sub>2</sub>O<sub>2</sub> and impairment in the activation of MPK4 by flagellin [14]. Genetic studies show that the *bir1* mutant phenotype is dependent on BAK1, EDS1, and PAD4 and loss-of-function mutations in these genes can partially suppress the autoimmune phenotype of *bir1* mutant, indicating that over-accumulation of SA is partially responsible for the autoimmune phenotype [14,15]. The kinase activity of BAK1 is required for its function in activation of defense responses in *bir1-1*.

SOBIR1 (suppressor of BIR1) was identified as a suppressor of *bir1-1* autoimmune phenotypes in a suppressor screening. Loss of function in SOBIR1 strongly suppresses cell death in *bir1-1*. Combining the *sobir1* and *pad4-1* mutations leads to suppression of all mutant phenotypes of *bir1-1*, suggesting that SOBIR1 functions in parallel with PAD4. SOBIR1 encodes an RLK with four extracellular LRRs and a cytoplasmic kinase domain [14]. BAK1 interacts with SOBIR1 only when BIR1 is absent [15–17]. In the absence of BIR1, inhibition of BAK1 by BIR1 is released and BAK1 forms an active receptor complex with SOBIR1, leading to cell death and defense responses [15]. In addition, BAK1 associates with the BIR1 and the copain-like proteins BONZAI1 (BON1)–BON3, which are required to suppress autoimmunity [18].

BIR2 is an inactive pseudokinase and a substrate of BAK1. It forms a constitutive complex with BAK1 to prevent it from interacting with FLS2. The kinase activity of BAK1 is required for BIR2–BAK1 interaction [19]. BIR2 is released from BAK1 after PAMP treatment and BIR2 controls BAK1–FLS2 complex formation in a ligand-dependent manner [19]. *bir2* mutant plants exhibit enhanced pathogen-associated molecular pattern (PAMP) responses but do not have the dwarf morphology like *bir1-1*. Unlike BIR2, BIR1 is an active kinase, and kinase activity is at least partially required for its function. flg22 treatment leads to dissociation of BIR2 from BAK1 and over-expression of BIR2 attenuates PAMP-triggered responses [19].

Although extensively studied in the model plant Arabidopsis, the investigations of RLKs in crop plants are limited. Using the BPMV-VIGS system, we have recently identified multiple positive and negative regulators of defense responses in soybean [20–25]. Here, using the same strategy, we identified *GmBIR1* as a negative regulator of defense responses in soybean. Silencing *GmBIR1* led to spontaneous cell death and constitutively activated defense responses. These autoimmune responses are highly correlated with the over-accumulation of both SA and H<sub>2</sub>O<sub>2</sub>. Consistent with the autoimmune phenotypes, the *GmBIR1*-silenced plants displayed a significantly increased resistance to both *Soybean mosaic virus* (SMV) and *Pseudomonas syringae* pv. *glycinea* (*Psg*). Taken together, our results indicate that *GmBIR1* plays a negative regulatory role in soybean immunity, and the function of BIR1 homologs is conserved across plant species.

## 2. Results

### 2.1. Silencing *Glyma.18g246400* Results in Stunted Stature and Spontaneous Cell Death in Soybean

Through BPMV-VIGS silencing approach, we successfully identified both positive and negative regulators of defense responses in soybean [20–25]. Using the same strategy, we found that when *Glyma.18g246400* was silenced, a significantly stunted stature (Figure 1A) and spontaneous cell death on the systemic leaves were observed for the silenced plants (Figure 1B). The cell death was further confirmed by Trypan blue staining, which specifically stains the dead cells. The massive blue patches were observed along the larger veins on the systemic leaves of the silenced plants but not on that of vector control plants (Compare Figure 1C,D). RT-PCR analysis confirmed that the transcript level of *Glyma.18g246400* was significantly reduced in the silenced plants (Figure 1E). Stunted stature and spontaneous cell death are the signature characteristics of the constitutively activated defense responses. Consistent with this, a significantly induced expression of the *PR1* gene was observed in the silenced plants (Figure 1F). These results indicated that *Glyma.18g246400* encodes a negative regulator of cell death and defense responses. Blast search with the full-length cDNA of *Glyma.18g246400* revealed that there is a duplicated gene in the soybean genome, *Glyma.09g246600*, which shares 95% identity with *Glyma.18g246400*. It has been reported that VIGS can simultaneously silence genes with a homology greater than 85% at the nucleotide level [26,27]. We confirmed that the silenced phenotype observed for the *Glyma.18g246400*-silenced plants was actually a result of co-silencing both *Glyma.18g246400* and *Glyma.09g246600* (Figure 1G). Both *Glyma.18g246400* and *Glyma.09g246600* share the highest homology with *Arabidopsis BIR1* (65%), we thus referred to these two genes as *GmBIR1a* and *GmBIR1b*, respectively. Because the *bir1* mutant in *Arabidopsis* displays a constitutive activated defense phenotype (Gao et al., 2009), our results indicate that the function of *BIR1* homologs is conserved in different plants species.

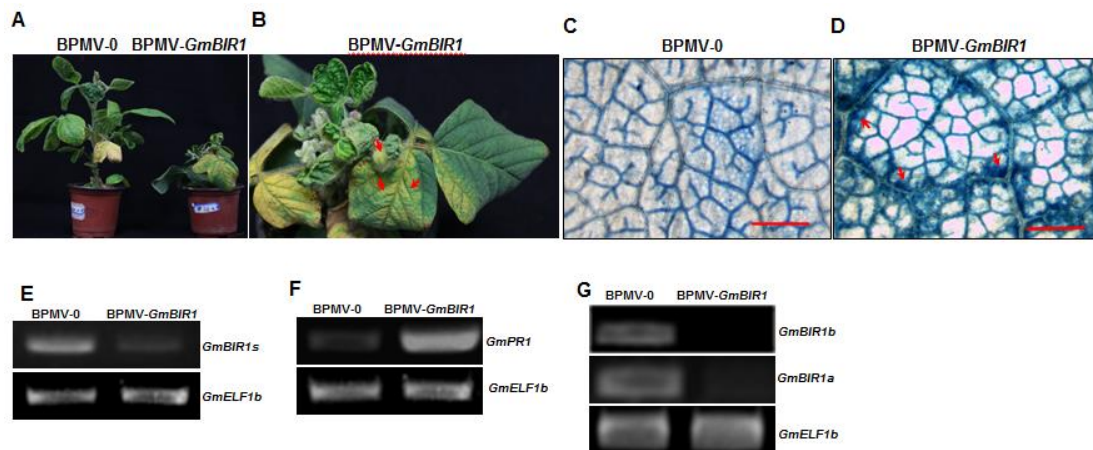


**Figure 1.** Silencing *GmBIR1* causes both local and systemic hypersensitive response (HR) cell death in soybean. (A) The phenotypes of vector control (BPMV-0) and *GmBIR1*-silenced (BPMV-*GmBIR1*) plants at 15 days post infection (dpi); (B) Massive cell death was observed on the systemic leaves of *GmBIR1*-silenced plants at 25 dpi. Red arrows point to the dead leaves; (C,D) Trypan Blue-stained systemic leaves from vector control (C) and *GmBIR1*-silenced plants (D). Red arrows point to the dead regions. Bar = 500  $\mu$ m; (E) RT-PCR result indicates that the *GmBIR1* transcript level was reduced in *GmBIR1*-silenced plants relative to the vector control plants; (F) RT-PCR result indicates that the *GmPR1* transcript level was increased in *GmBIR1*-silenced plants relative to the vector control plants; (G) RT-PCR result indicates that the *GmBIR1a* and *GmBIR1b* transcript level were both reduced in *GmBIR1*-silenced plants relative to the vector control plants. Each experiment was repeated at least twice. Each experiment consisted of 3 replicates and at least 3 plants were used in each replicate.

### 2.2. Both SA and H<sub>2</sub>O<sub>2</sub> Are Over-Accumulated in the GmBIR1-Silenced Plants

SA is a key hormone that positively regulates defense responses against biotrophic pathogens and is over-accumulated in the plants with activated defense responses [20,28]. To examine whether SA over-accumulation occurred in *GmBIR1*-silenced plants, both free SA and bound SA were quantified, and the levels of free SA and bound SA were 2.46- and 4.1-fold higher in the *GmBIR1*-silenced plants than in BPMV-0 control plants, respectively (Figure 2A,B). The over-accumulated level of SA suggests that SA is involved in the constitutively activated defense responses observed in *GmBIR1*-silenced plants.

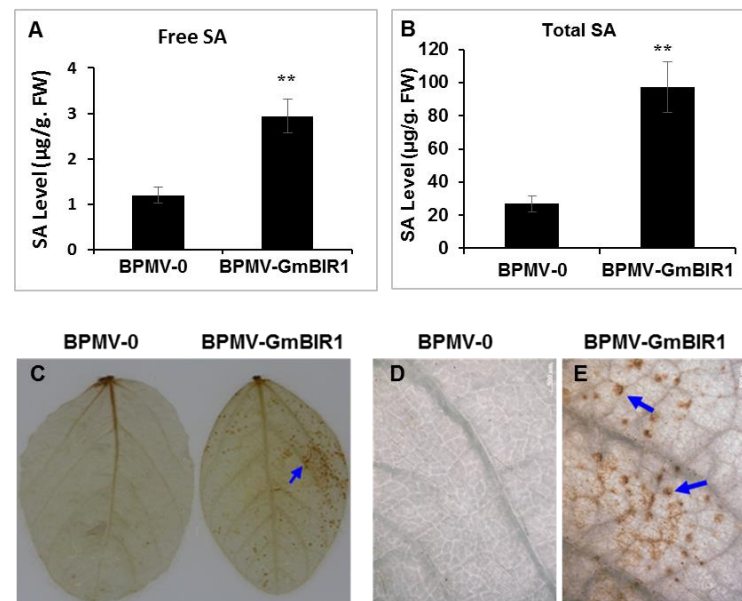


**Figure 2.** Elevated accumulation of SA and H<sub>2</sub>O<sub>2</sub> in *GmBIR1*-silenced plants. (A,B) Free SA (A) and Total SA (B) levels were quantified in *GmBIR1*-silenced and BPMV-0 empty vector control plants at 20 days post BPMV inoculation. Error bars represent SD for three independent samples. Asterisks indicate significant differences from the control (\*\*,  $p < 0.01$ , Student's  $t$  test). FW, fresh weight. (C) Presence of H<sub>2</sub>O<sub>2</sub> in soybean leaves visualized by staining with DAB. (D,E) The images taken under the stereomicroscope from part of the regions shown in C, Bar = 500 µm. Oxidized DAB formed a reddish-brown deposit. (Examples of these deposits are indicated by the blue arrows).

H<sub>2</sub>O<sub>2</sub> is a potent trigger of cell death [29,30] and H<sub>2</sub>O<sub>2</sub> is over-accumulated in the plants with activated defense responses [20,23]. To examine if H<sub>2</sub>O<sub>2</sub> is over-accumulated in the *GmBIR1*-silenced plants, the leaves collected from both vector control plants and the *GmBIR1*-silenced plants were stained with 3,3-diaminobenzidine (DAB) [31,32]. More intense brown spots were observed on the leaves of the *GmBIR1*-silenced plants compared to the BPMV-0 control plants (Figure 2C), indicating that the cell death observed in the *GmBIR1*-silenced plants was correlated with increased level of H<sub>2</sub>O<sub>2</sub> accumulation.

### 2.3. Silencing *GmBIR1* Enhances Resistance against SMV and *Pseudomonas syringae* pv. *glycinea* (Psg), R4 Strain

Activated defense responses are usually correlated with enhanced disease resistance [20–25]. To examine whether disease resistance is enhanced in *GmBIR1*-silenced plants, SMV strain N tagged with the GUS marker protein (SMV-N-GUS) [33] was inoculated via biolistic bombardment onto three individual leaves collected from both the vector control plants and the *GmBIR1*-silenced plants. Both the size of the GUS foci and the intensity of GUS staining reflect viral infectivity. At 5 days post inoculation (dpi), the SMV-N-GUS infection was visualized by GUS staining. The GUS infection foci were easily seen on the vector control leaves (Figure 3A, left panels; Figure 3B). However, the GUS spots on the *GmBIR1*-silenced plants were much smaller and only visible under a dissecting

microscopy (Figure 3C). The average diameter of the GUS foci formed on the vector control leaves was four-fold of those formed on the *GmBIR1*-silenced leaves (Figure 3D). This result indicates that silencing *GmBIR1* leads to increased resistance against SMV.

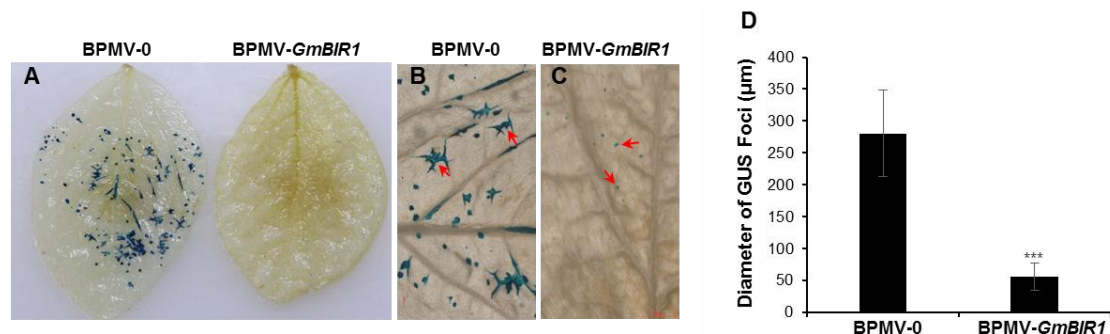


**Figure 3.** Silencing *GmBIR1* enhances the resistance of soybean plants to SMV. At 18 dpi with BPMV-0 or BPMV-*GmBIR1*, SMV-N-GUS was biolistically delivered onto the detached leaves of silenced and non-silenced plants. At 5 dpi with SMV-N-GUS, the replication and movement of SMV-N-GUS in the biolistically inoculated leaves was detected by GUS staining. The GUS foci were counted and measured. (A) The distribution of SMV-N-GUS foci on the leaves of BPMV-0 and BPMV-*GmBIR1* plants. (B,C) Infection foci of SMV-N-GUS on the leaves of BPMV-0 and BPMV-*GmBIR1* plants. Bar = 2000 µm. (D) Comparison of the diameters of SMV-N-GUS foci on the leaves of BPMV-0 and BPMV-*GmBIR1* plants. Error bars represent SD of the diameters of at least 30 GUS foci measured on each of three independent leaves (at least 90 foci). Asterisks indicate a significant difference from the control (\*\*\*,  $p < 0.001$ , Student's *t* test). This experiment was repeated 3 times with similar results.

We reported that silencing *GmFLS2* compromises soybean resistance against *Pseudomonas syringae* pv. *glycinea* (*Psg*) R4 [24]. To test the effect of *GmBIR1* silencing on *Psg* infection, we inoculated the BPMV-0 control plants and the *GmBIR1*-silenced plants with *Psg*. At 4- and 6-dpi, the colony forming unit of *Psg* on the vector control leaves was significantly higher than on that of the *GmBIR1*-silenced leaves (Figure 4). Together, these results clearly show that silencing *GmBIR1* enhances resistance of soybean plants against two totally different types of pathogens, SMV and *Psg*.

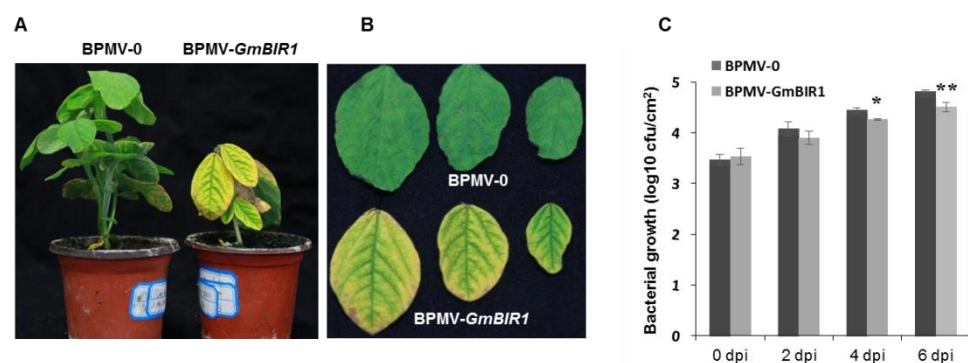


**Figure 4.** Silencing *GmBIR1* enhanced the resistance of soybean plants to *Pseudomonas syringae* pv. *glycinea* (*Psg*) R4. (A) Comparison of the vector control plants and the *GmBIR1*-silenced plants 4 days after spraying *Psg* suspension; (B) Comparison of the leaves from the vector control plants and the *GmBIR1*-silenced plants 4 days after spraying *Psg*; (C) Comparison of the colony forming unit (cfu) between the vector control plants and the *GmBIR1*-silenced plants after different days of *Psg* infection. \* and \*\* represent  $p < 0.05$  and  $0.01$ , respectively (Student's *t*-test). This experiment was repeated 2 times with similar results.

#### 2.4. The Activated Defense Responses in *GmBIR1*-Silenced Plants Are Independent of *GmMPK3/6* Activation

Activation of MAPK signaling pathway is one of the signature hallmarks of activated defense responses [34]. To test whether the activated MAPK signaling pathway contributes to the activated defense responses and enhanced disease resistance observed in *GmBIR1*-silenced plants (Figures 1–4), the activation of *GmMPK3* and *GmMPK6* in response to flg22 was examined both in vector control plants and *GmBIR1*-silenced plants using the Phospho-p44/42 MAP Erk1/2 antibody that recognizes phosphorylation of Arabidopsis and soybean MPK3/4/6 at the sites corresponding to threonine (T) 202/tyrosine (Y) 204 of human (*Homo sapiens*) p44 MAPK [23,24,35]. Contrary to our expectation, activation of both *GmMPK3* and *GmMPK6* by flg22 was significantly reduced in *GmBIR1*-silenced plants compared to vector control plants (Figure 4), indicating that the activated defense responses observed in the *GmBIR1*-silenced plants are independent of *GmMPK3/6* activation.

#### 2.5. *GmBIR1* Is Localized at the Plasma Membrane (PM) and in the Nucleus

RLKs normally function at the PM. To investigate the subcellular location of *GmBIR1*, the full-length *GmBIR1a* was fused to the C-terminus of GFP and transiently co-expressed in *N. benthamiana* leaves with a PM marker, *AtCBL1-mCherry*, via agroinfiltration. As shown in Figures 5 and 6, GFP-*GmBIR1* was not only co-localized with *AtCBL1-mCherry* but also presented in the nucleus, indicating that *GmBIR1* has dual subcellular localizations at the PM and in the nucleus.

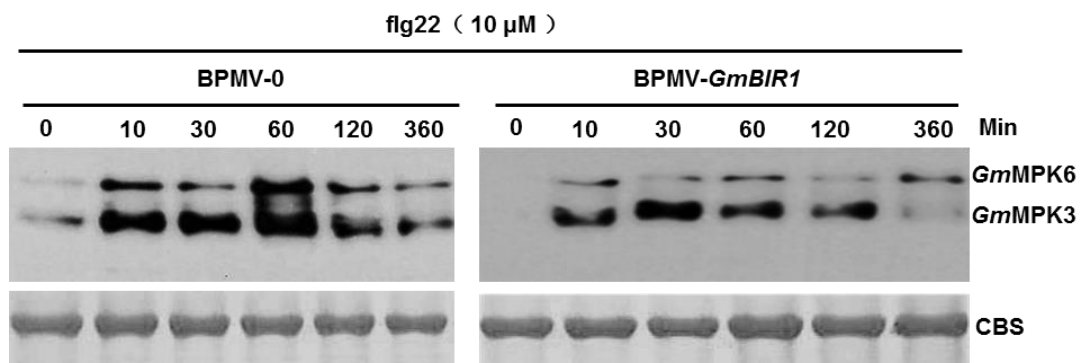


**Figure 5.** Silencing *GmBIR1* reduces the activation of *GmMPK3/GmMPK6* in response to flg22 treatment. Leaf discs from indicated soybean plants were incubated on moist filter paper for 24 h to allow recovery from wounding before being treated with 10  $\mu$ M flg22 or diluted DMSO. The kinase activities were detected by Western blotting using Phospho-p44/p42 MAP Erk1/2 antibody. Coomassie Blue-stained gel (CBS) used as loading controls. The experiment was repeated 3 times with similar results.

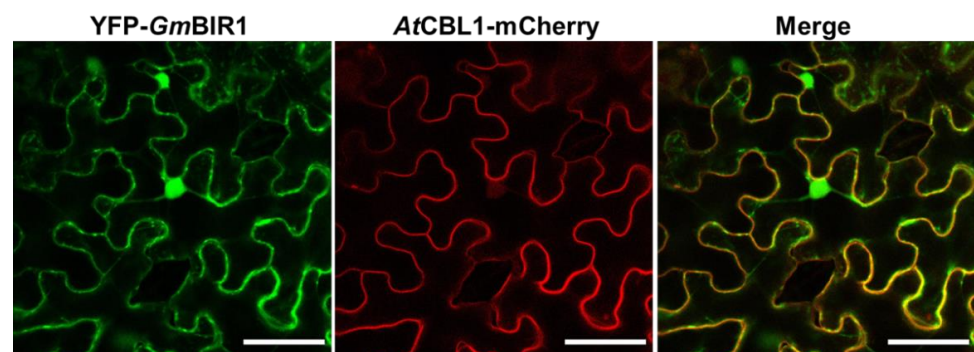


**Figure 6.** The subcellular localization of GFP-*GmBIR1*. The GFP-*GmBIR1* localizes both at plasma membrane (PM) and in the nucleus. The PM-localized protein *AtCBL1-mCherry* was used as a control. Bar = 50  $\mu$ m. This experiment was repeated 3 times with similar results.

### 3. Discussion

#### 3.1. The Function of BIR1 Homologs Is Conserved from Different Plant Species

It has been reported that the extensive cell death, induction of *PR* genes, enhanced accumulation of SA and H<sub>2</sub>O<sub>2</sub>, impaired activation of MPK4, and enhanced resistance to different pathogens were observed for Arabidopsis *bir1-1* mutant [14,15,36–38]. Similarly, spontaneous cell death, constitutively activated autoimmune responses (including induced *PR* gene expression), accumulated levels of both SA and H<sub>2</sub>O<sub>2</sub>, and enhanced disease resistance to both viral and bacterial pathogens were also observed for the *GmBIR1*-silenced soybean plants (Figures 1–3). The phenotypic reminiscence between *bir1-1* mutant and the *GmBIR1*-silenced plants strongly indicate that the functions of BIR1 homologs are highly conserved across plant species in negatively regulating cell death and immunity. Given that cell death occurs in *bir1-1* mutants even under sterile conditions, BIR1 may not function in perception of PAPMs (pathogen-associated molecular patterns).

#### 3.2. The Constitutively Activated Cell Death and Defense Responses in *GmBIR1*-Silenced Plants Is A Result of Co-Silencing of Both *GmBIR1a* and *GmBIR1b*

Soybean is a paleopolyploid and 75% of genes in its genome contain at least two copies [39]. Consistent with this, there are two *GmBIR1* genes, *GmBIR1a* and *GmBIR1b*, in the soybean genome. The open reading frame sequences of *GmBIR1a* and *GmBIR1b* share 95% identity at the nucleotide level. The DNA fragment used for *GmBIR1* silencing contains four stretches of sequences with 100% identity between *GmBIR1a* and *GmBIR1b* that could potentially generate siRNAs of >20 nt in length (Supplementary Figure S1). Therefore, both *GmBIR1a* and *GmBIR1b* were silenced using the same construct (Figure 1G). The autoimmune phenotype of the *GmBIR1*-silenced plants (Figure 1B) actually is a result of co-silencing of both *GmBIR1a* and *GmBIR1b*. We have previously shown that multiple copies of *GmMPK4*, *GmMPK6*, *GmMEKK1*, *GmFLS2*, and *GmATG2* genes could be successfully co-silenced using a single BPMV-VIGS construct [20,22–25]. Given that soybean is polyploidy and is recalcitrant to transformation, VIGS is currently one of the most efficient approaches to interrogate gene functions in soybean [26,27].

#### 3.3. Does the Autoimmunity Observed in *GmBIR1*-Silenced Plants Result from Activated PTI or Activated ETI?

Activation of either PTI or ETI results in autoimmune responses, although the autoimmune responses resulting from ETI are much stronger and last longer than those resulting from PTI [1]. Structure analysis indicates that Arabidopsis BIR1 and BAK1 directly interact with each other through their ecto-LRR domains [36]. Under no-elicited conditions, BIR1<sup>LRR</sup>-BAK1<sup>LRR</sup> interaction sequesters BAK1 and prevents formation of a signal competent complex with FLS2. In the presence of flg22, flg22-bound FLS2<sup>LRR</sup> outcompetes BIR1<sup>LRR</sup> for binding to BAK1<sup>LRR</sup> from the BIR1<sup>LRR</sup>-BAK1<sup>LRR</sup> complex and forms a signaling competent flg22-FLS2<sup>LRR</sup>-BAK1<sup>LRR</sup> complex [36]. Based on this structural study, BIR1 functions to keep BAK1-mediated cell death signaling under tight control, thus preventing undesired autoimmunity, and therefore, it is possible that the autoimmunity in *bir1-1* or *GmBIR1*-silenced plants is a result of activation of BAK1-mediated PTI. Our *Psg* infection assay supported this possibility (Figure 4). However, inconsistent with this possibility, the flg22-induced activation of *GmMPK3* and *GmMPK6*, which is a hallmark event of activated PTI (Meng et al., 2013), was significantly reduced in *GmBIR1*-silenced plants relative to vector control plants (Figure 4), and the activation of MPK3 and MPK6 in the Arabidopsis *bir1-1* mutant is unchanged compared to WT Col-0 [14]. Therefore, it is still unclear whether the autoimmune responses observed in *bir1-1* or *GmBIR1*-silenced plants are solely due to activated PTI, reflecting the complexity of the involvement of BIR1 in plant immunity.

Several lines of evidence indicate that autoimmune responses in *bir1-1* or the *GmBIR1*-silenced plants could result from misactivation of R proteins. Firstly, loss function of BIR1 in Arabidopsis leads to the impairment in the activation of MPK4 by flagellin [14].

The autoimmune phenotype of *bir1-1* could be the consequence of the impaired MPK4 activation given that Arabidopsis MEKK1-MKK1/2-MPK4 signaling module negatively regulates the activation of the R proteins SUMM2 and SMN1/RPS6 [40–42]. Misactivation of SUMM2 and SMN1/RPS6 result from mutations in MEKK1-MKK1/2-MPK4 pathway leads to autoimmune responses [40,42]. However, *GmMPK4* activity cannot be induced either by flg22 or SA, regardless of concentration and duration of treatments [23]. Therefore, it is unclear whether *GmMPK4* plays a similar role as its counterpart in Arabidopsis. As the *GmMPK4* activation is also not observed in the vector control plants (Figure 4 and [23]), it is unlikely that the *GmBIR1*-silenced phenotypes are related to *GmMPK4* function. Secondly, in *Arabidopsis thaliana*, the copain-like protein BONZAI1 (BON1) interacts physically with and phosphorylates BIR1 and *bir1-1* mutant is partially suppressed by loss of function mutation in the resistance gene *SNC1* [18]. Thirdly, the autoimmune phenotype of *bir1-1* can be partially suppressed by elevated temperatures [18], which is a characteristic feature of R protein-mediated responses [43,44]. Lastly, the autoimmune phenotype of *bir1-1* is rescued by the loss of function of EDS1 and PAD4 [14], two key players in TIR type of R protein activation [45]. These results strongly suggest that the autoimmune phenotype of the *bir1-1* mutant is a result of misactivated R protein(s). Therefore, it is possible that BIR1 might participate in both PTI and ETI through interacting with different proteins, and the autoimmune responses observed in *bir1-1* and *GmBIR1*-silenced plants could be combined effects of activated PTI and ETI. The facts that RLKs/RLPs are required for NLR-mediated immunity [46] and RLKs/RLPs and NLRs mutually potentiate each other [47] support the idea that BIR1 may participate in both PTI and ETI.

#### 3.4. Is the Enhanced Resistance of *GmBIR1*-Silenced plants to SMV SA-Dependent?

The enhanced resistance of *GmBIR1*-silenced plants against *Psg* could be attributed to the increased accumulation of both SA and H<sub>2</sub>O<sub>2</sub> (Figure 2) and is thus SA-dependent. The enhanced SMV resistance in *GmBIR1*-silenced plants may not be solely due to increased accumulation of both SA and H<sub>2</sub>O<sub>2</sub>. In Arabidopsis, Guzman-Benito et al. [38] reported that the enhanced resistance of *bir1-1* to *Tobacco rattle virus* (TRV) is independent of cell death or SA defense priming. The expression of Arabidopsis *BIR1* is regulated both at TGS and PTGS level by RNA silencing pathway [38]. A threshold level of *BIR1* expression must be properly maintained and an expression beyond the threshold level (either too high or too low) triggers autoimmunity. Whether the enhanced resistance of *GmBIR1*-silenced plants to SMV is uncoupled from the cell death needs to be further investigated.

## 4. Materials and Methods

### 4.1. Plant Materials

Seeds of soybean (*Glycine max* ‘Williams 82’) used in this study were harvested from greenhouse-grown plants previously indexed for the absence of BPMV and SMV [48,49]. Soybean plants were grown in a growth chamber at 22 degrees with a photoperiod of 16 h.

### 4.2. Flg22 Peptides

The flg22 peptide was synthesized by HuaBio (Hangzhou, China).

### 4.3. BPMV-Mediated VIGS

BPMV strains, BPMV VIGS constructs, and inoculation of soybean seedlings with DNA-based BPMV constructs via biolistic particle bombardments using a Biolistic PDS-1000/He system (Bio-Rad Laboratories, Hercules, CA, USA) have been described previously [48]. The orthologs of Arabidopsis *BIR1* in the soybean genome were identified by BLASTN in phytosome databases. The primers used for construction of the BPMV-*GmBIR1* (*Glyma.18g246400.1*) are:

*GmBIR1*-F: 5'-aagGGATCCCTCACTGGTCAAATTCCTGCTA-3'  
*GmBIR1*-R: 5'-ttgGGTACCCAGGGTCTCTTCCTTCTTCTCA-3'

The underlined sequences are *Bam*H I and *Kpn* I restriction sites, respectively, which were used for directional cloning of the PCR fragment into the BPMV VIGS (IA-D35). The letter C in bold indicates an extra nucleotide in reverse primers needed to maintain the correct open reading frame with BPMV genome.

#### 4.4. RNA Isolation and RT-PCR

RNA isolation and RT-PCR were performed as described elsewhere [50]. The RNA samples extracted were treated with DNaseI according to the manufacturer's instructions (Invitrogen, Carlsbad, CA, USA). Primers used for RT-PCR in this study are:

*GmELF1b*-F: 5'- ACCGAAGAGGGCATCAAATCCC -3'

*GmELF1b*-R: 5'- CTCAACTGTCAAGCGTTCCTC -3'

*GmBIR1*-full-F: 5'- ATAGGAAGAAGGAAGAGGACC -3'

*GmBIR1*-full-R: 5'- TTTAGGAGTAGCCACCAAAGT -3'

*GmBIR1a*-F: 5'- GACTTGCTCAATATCCCAGGATAAGT-3'

*GmBIR1a*-R: 5'- TGTTGAGATTCCTGTAATCTCTTAACCAT -3'

*GmBIR1b*-F: 5'- TACTTCCTCAATATCCCAGGTGG -3'

*GmBIR1b*-R: 5'- TATTGAGATTCCTGCAATCTCTTGAC -3'.

The *GmBIR1a*-full primers were used for amplifying the full-length cDNA and the *GmBIR1a* and *GmBIR1b* primers are used for determining the specific transcript levels of the *GmBIR1a* and *GmBIR1b*, respectively.

#### 4.5. Trypan Blue Staining

Cell death was detected specifically by trypan blue staining solution as described by [18]. At 18 dpi with BPMV vector only (BPMV-0) or BPMV-*GmBIR1* constructs, second fully expanded soybean trifoliolate leaves counting from the top were detached. The detached leaves were placed in trypan blue staining solution (10 mL glycerol, 10 mL lactic acid, 10 mL water, 10 mg trypan blue powder and 10 g phenol) and boiled for 1–1.5 min. The stained leaves were cleared using tap water and then dipped in the chloral hydrate solution in the shaker overnight to remove the non-specific stains. Images were captured using a stereo microscope (Olympus SZH10, Center Valley, PA, USA).

#### 4.6. SA Quantification

SA was quantified using an Agilent 1260 HPLC system (Agilent Technologies) with a diode array detector and a fluorescence detector and a column as described previously [51]. The column was a 4.6-by-75-mm Zorbax SB-C18 with a mobile phase comprising sodium acetate (0.2 M, pH 5.5) and methanol with a series of concentration gradients. The initial methanol gradient was maintained at 3% (*v/v*) for 12 min, linearly increased to 7% (*v/v*) at 12.5 min and maintained until 38 min at a flow rate of 0.8 mL min<sup>-1</sup> throughout the process. After 1 min, the initial reaction conditions were restored and the system needed to be equilibrated for 7 min before the next injection. Total SA from the sample treated with  $\beta$ -Glucosidase and free SA were detected with a 296 nm excitation wavelength and 410 nm emission wavelength. The concentration was calculated by determining the HPLC peak area according to a standard curve.

#### 4.7. H<sub>2</sub>O<sub>2</sub> Detection by DAB Staining

H<sub>2</sub>O<sub>2</sub> was detected by an endogenous peroxidase-dependent in situ histochemical staining procedure using DAB (Sigma-Aldrich, St. Louis, MO, USA) [32]. Detached leaves were placed in a solution containing 1 mg mL<sup>-1</sup> DAB (pH 5.5) for 2 h. The leaves were cleared by boiling in 96% (*v/v*) ethanol for 10 min. H<sub>2</sub>O<sub>2</sub> production was visualized as a reddish-brown precipitate on the cleared leaves [32].

#### 4.8. Inoculation of *Pseudomonas Syringae* pv. *Glycinea* (Psg) onto the Leaves of Soybean Plants

*Psg* growth assay was performed as described by [24]. *Psg* was cultivated at 28 degrees until OD = 1.3. The bacterial culture was centrifuged at 3000 rpm for 10 min and the

pellet was re-suspended in double-distilled water with an OD = 1. The vector control or *GmBIR1*-silenced plants were thoroughly and evenly sprayed with the re-suspended bacterial solution on both upsides and downsides of the leaves. The sprayed plants were immediately covered with transparent plastic bags for at least 24 h.

#### 4.9. SMV-N-GUS Inoculation, GUS Staining, and GUS Foci Measurements

At 18 dpi with BPMV vector only (BPMV-0) or BPMV-*GmBIR1* constructs, second fully expanded soybean trifoliolate leaves counting from the top were detached and biolistically inoculated with SMV-N-GUS [33,48]. Following SMV-N-GUS inoculation, the detached leaves were put into petri dishes with moist filter papers and kept on a lighted growth shelf for 5 days before GUS staining. GUS staining was performed as described by [52]. Photographs of the leaves with GUS foci were taken using a stereo microscope (Olympus SZH10, Center Valley, PA, USA). The numbers of GUS foci were counted, and the diameters of GUS foci were measured using Soft Image System analysis (IA Package; Olympus).

#### 4.10. Western Blot Analysis for Detecting Phosphorylated MPKs

Protein was extracted from soybean leaf tissues using extraction buffer (50 mM Tris-MES pH 8.0, 0.5 M sucrose, 1 mM MgCl<sub>2</sub>, 10 mM EDTA, 5 mM DTT) with protease inhibitor cocktail S8830 (Sigma-Aldrich, St. Louise, MO, USA) added as described by [23]. The extract was centrifuged at 12,000 rpm at 4 °C for 30 min and the supernatant was collected. For immunoblotting, the extracted proteins were separated by SDS-PAGE (10% acrylamide gel) and transferred to PVDF membrane (Millipore, Billerica, MA, USA) by semi-dry electro-transfer (Bio-Rad, Hercules, CA, USA). The membrane was blocked in 1 × TBST buffer containing 5% milk powder for 2 h. After washing, the membrane was further incubated with anti-Phospho-p44/p42 MAPK (anti-pTEpY) diluted at 1:3000 (Cell Signaling Technology, Danvers, MA, USA), followed by incubation with secondary antibody diluted at 1:7500. The bands were visualized by incubating with chemiluminescent HRP substrate (Millipore, Billerica, MA, USA).

#### 4.11. Subcellular Localization of *GmBIR1*

The *GmBIR1* (Glyma.18g246400.1) open reading frame was amplified by RT-PCR from total RNA extracted from cv Williams 82 soybean plants using the following primers:

*GmBIR1*-PGDG-F-HinDIII: 5'-**AAGCTT**ATGAAGATGTTTATGGGGTGGC-3'

*GmBIR1*-PGDG-R-BamHI: 5'-**GGATCCT**CAATCATGTCCCTCTCGAG-3'

The letters in bold represent the cleavage sites for different restriction enzymes.

The RT-PCR products were firstly double digested with HindIII + BamHI and subsequently cloned into the PGDG vector [53] to generate the GFP-*GmBIR1* fusion construct. These fusion constructs and the *AtCBL1*-mCherry construct (membrane marker) were coinfiltrated into *N. benthamiana* leaves as described by [50]. Images were captured with a confocal laser-scanning microscope (Leica TCS SP5 AOBS, Wetzlar, Germany).

**Supplementary Materials:** The following supporting information can be downloaded at: <https://www.mdpi.com/article/10.3390/ijms23137450/s1>.

**Author Contributions:** J.-Z.L. designed the experiments and wrote the original draft; D.-D.L., H.-J.L., H.S.M., M.-Y.Y., X.-Y.D., C.-L.Z. and S.-N.T. performed the experiments; J.-Z.L. and D.-D.L. prepared figures. All authors have read and agreed to the published version of the manuscript.

**Funding:** This research was funded by the National Natural Science Foundation of China (grant numbers 32170761 and 31571423 to J.Z.L.).

**Informed Consent Statement:** No applicable.

**Data Availability Statement:** No applicable.

**Acknowledgments:** We thank Steven A. Whitham and John Hill for providing the BPMV-VIGS system, *Pseudomonas syringae* pv. *glycinea* R4 strain and SMV-N-GUS construct.

**Conflicts of Interest:** The authors declare no conflict of interest.

## References

- Jones, J.D.; Dangl, J.L. The plant immune system. *Nature* **2006**, *444*, 323–329. [[CrossRef](#)] [[PubMed](#)]
- Shiu, S.H.; Bleecker, A.B. Receptor-like kinases from Arabidopsis form a monophyletic gene family related to animal receptor kinases. *Proc. Natl. Acad. Sci. USA* **2001**, *98*, 10763–10768. [[CrossRef](#)] [[PubMed](#)]
- Jamieson, P.A.; Shan, L.; He, P. Plant cell surface molecular cypher: Receptor-like proteins and their roles in immunity and development. *Plant Sci.* **2018**, *274*, 242–251. [[CrossRef](#)] [[PubMed](#)]
- Boller, T.; Felix, G. A renaissance of elicitors: Perception of microbe-associated molecular patterns and danger signals by pattern-recognition receptors. *Annu. Rev. Plant Biol.* **2009**, *60*, 379–406. [[CrossRef](#)] [[PubMed](#)]
- Gómez-Gómez, L.; Boller, T. FLS2: An LRR Receptor-like Kinase Involved in the Perception of the Bacterial Elicitor Flagellin in Arabidopsis. *Mol. Cell* **2009**, *5*, 1003–1011. [[CrossRef](#)]
- Zipfel, C.; Kunze, G.; Chinchilla, D.; Caniard, A.; Jones, J.D.; Boller, T.; Felix, G. Perception of the Bacterial PAMP EF-Tu by the Receptor EFR Restricts Agrobacterium-Mediated Transformation. *Cell* **2006**, *125*, 749–760. [[CrossRef](#)]
- Li, J.; Wen, J.; Lease, K.A.; Doke, J.T.; Tax, F.E.; Walker, J.C. BAK1, an Arabidopsis LRR Receptor-like Protein Kinase, Interacts with BRI1 and Modulates Brassinosteroid Signaling. *Cell* **2002**, *110*, 213–222. [[CrossRef](#)]
- Nam, K.H.; Li, J. BRI1/BAK1, a Receptor Kinase Pair Mediating Brassinosteroid Signaling. *Cell* **2002**, *110*, 203–212. [[CrossRef](#)]
- Chinchilla, D.; Zipfel, C.; Robatzek, S.; Kemmerling, B.; Nürnberger, T.; Jones, J.D.G.; Felix, G.; Boller, T. A flagellin-induced complex of the receptor FLS2 and BAK1 initiates plant defence. *Nature* **2007**, *448*, 497–500. [[CrossRef](#)]
- Heese, A.; Hann, D.R.; Gimenez-Ibanez, S.; Jones, A.M.; He, K.; Li, J.; Schroeder, J.I.; Peck, S.C.; Rathjen, J.P. The receptor-like kinase SERK3/BAK1 is a central regulator of innate immunity in plants. *Proc. Natl. Acad. Sci. USA* **2007**, *104*, 12217–12222. [[CrossRef](#)]
- Roux, M.; Schwessinger, B.; Albrecht, C.; Chinchilla, D.; Jones, A.; Holton, N.; Malinovskiy, F.G.; Tör, M.; de Vries, S.; Zipfel, C. The Arabidopsis leucine-rich repeat receptor-like kinase BAK1/SERK3 and BKK1/SERK4 are required for the innate immunity to hemibiotrophic and biotrophic pathogens. *Plant Cell* **2011**, *23*, 2440–2455. [[CrossRef](#)] [[PubMed](#)]
- Macho, A.P.; Schwessinger, B.; Ntoukakis, V.; Brutus, A.; Segonzac, C.; Roy, S.; Kadota, Y.; Oh, M.H.; Sklenar, J.; Derbyshire, P.; et al. A bacterial tyrosine phosphatase inhibits plant pattern recognition receptor activation. *Science* **2014**, *343*, 1509–1512. [[CrossRef](#)] [[PubMed](#)]
- Couto, D.; Zipfel, C. Regulation of pattern recognition receptor signalling in plants. *Nat. Rev. Immunol.* **2016**, *16*, 537–552. [[CrossRef](#)] [[PubMed](#)]
- Gao, M.; Wang, X.; Wang, D.; Xu, F.; Ding, X.; Zhang, Z.; Bi, D.; Cheng, Y.T.; Chen, S.; Li, X.; et al. Regulation of cell death and innate immunity by two receptor-like kinases in Arabidopsis. *Cell Host Microbe* **2009**, *6*, 34–44. [[CrossRef](#)] [[PubMed](#)]
- Liu, Y.; Huang, X.; Li, M.; He, P.; Zhang, Y. Loss-of-function of Arabidopsis receptor-like kinase BIR1 activates cell death and defense responses mediated by BAK1 and SOBIR1. *New Phytol.* **2016**, *212*, 637–645. [[CrossRef](#)] [[PubMed](#)]
- Liebrand, T.W.; van den Berg, G.C.; Zhang, Z.; Smit, P.; Cordewener, J.H.; America, A.H.; Sklenar, J.; Jones, A.M.; Tameling, W.I.; Robatzek, S.; et al. Receptor-like kinase SOBIR1/EVR interacts with receptor-like proteins in plant immunity against fungal infection. *Proc. Natl. Acad. Sci. USA* **2013**, *110*, 10010–10015. [[CrossRef](#)]
- Liebrand, T.W.; van den Burg, H.A.; Joosten, M.H. Two for all: Receptor-associated kinases SOBIR1 and BAK1. *Trends Plant Sci.* **2014**, *19*, 123–132. [[CrossRef](#)]
- Wang, Z.; Meng, P.; Zhang, X.; Ren, D.; Yang, S. BON1 interacts with the protein kinases BIR1 and BAK1 in modulation of temperature-dependent plant growth and cell death in Arabidopsis. *Plant J.* **2011**, *67*, 1081–1093. [[CrossRef](#)]
- Halter, T.; Imkamp, J.; Mazzotta, S.; Wierzbka, M.; Postel, S.; Bücherl, C.; Kiefer, C.; Stahl, M.; Chinchilla, D.; Wang, X.; et al. The leucine-rich repeat receptor kinase BIR2 is a negative regulator of BAK1 in plant immunity. *Curr. Biol.* **2014**, *24*, 134–143. [[CrossRef](#)]
- Liu, J.Z.; Horstman, H.D.; Braun, E.; Graham, M.A.; Zhang, C.; Navarre, D.; Qiu, W.L.; Lee, Y.; Nettleton, D.; Hill, J.H.; et al. Soybean homologs of MPK4 negatively regulate defense responses and positively regulate growth and development. *Plant Physiol.* **2011**, *157*, 1363–1378. [[CrossRef](#)]
- Liu, J.Z.; Whitham, S.A. Overexpression of a soybean nuclear-localized type III DnaJ domain-containing HSP40 reveals its roles in cell death and disease resistance. *Plant J.* **2013**, *74*, 110–121. [[CrossRef](#)] [[PubMed](#)]
- Liu, J.Z.; Braun, E.; Qiu, W.L.; Shi, Y.F.; Marcelino-Guimarães, F.C.; Navarre, D.; Hill, J.H.; Whitham, S.A. Positive and negative roles for soybean MPK6 in regulating defense responses. *Mol. Plant Microbe Interact.* **2014**, *27*, 824–834. [[CrossRef](#)] [[PubMed](#)]
- Xu, H.; Zhang, C.; Li, Z.C.; Wan, Z.R.; Jiang, X.X.; Tian, S.N.; Braun, E.; Mei, Y.; Qiu, W.L.; Li, S.; et al. The MAPK kinase GmMEKK1 regulates cell death and defense responses. *Plant Physiol.* **2018**, *178*, 907–922. [[CrossRef](#)] [[PubMed](#)]
- Tian, S.N.; Liu, D.D.; Zhong, C.L.; Xu, H.Y.; Yang, S.; Fang, Y.; Ran, J.; Liu, J.Z. Silencing *GmFLS2* enhances the susceptibility of soybean to bacterial pathogen through attenuating the activation of *GmMAPK* signaling pathway. *Plant Sci.* **2019**, *292*, 110386. [[CrossRef](#)]

25. Hashimi, S.M.; Wu, N.N.; Ran, J.; Liu, J.Z. Silencing Autophagy-Related Gene 2 (ATG2) Results in Accelerated Senescence and Enhanced Immunity in Soybean. *Int. J. Mol. Sci.* **2021**, *22*, 11749. [[CrossRef](#)]
26. Liu, J.Z.; Graham, M.A.; Pedley, K.F.; Whitham, S.A. Gaining insight into soybean defense responses using functional genomics approaches. *Brief. Funct. Genom.* **2015**, *14*, 283–290. [[CrossRef](#)]
27. Liu, J.Z.; Fang, Y.; Pang, H. The current status of the soybean-soybean mosaic virus (SMV) pathosystem. *Front. Microbiol.* **2016**, *7*, 1906. [[CrossRef](#)]
28. Petersen, M.; Brodersen, P.; Naested, H.; Andreasson, E.; Lindhart, U.; Johansen, B.; Nielsen, H.B.; Lacy, M.; Austin, M.J.; Parker, J.E.; et al. Arabidopsis map kinase 4 negatively regulates systemic acquired resistance. *Cell* **2000**, *103*, 1111–1120. [[CrossRef](#)]
29. Lamb, C.; Dixon, R.A. The oxidative burst in plant disease resistance. *Annu. Rev. Plant Physiol. Plant Mol. Biol.* **1997**, *48*, 251–275. [[CrossRef](#)]
30. Delledonne, M.; Xia, Y.; Dixon, R.A.; Lamb, C. Nitric oxide functions as a signal in plant disease resistance. *Nature* **1998**, *394*, 585–588. [[CrossRef](#)]
31. Thordal-Christensen, H.; Zhang, Z.G.; Wei, Y.D.; Collinge, D.B. Subcellular localization of H<sub>2</sub>O<sub>2</sub> in plants: H<sub>2</sub>O<sub>2</sub> accumulation in papillae and hypersensitive response during the barley-powdery mildew interaction. *Plant J.* **1997**, *11*, 1187–1194. [[CrossRef](#)]
32. Ren, D.; Yang, H.; Zhang, S. Cell death mediated by MAPK is associated with hydrogen peroxide production in Arabidopsis. *J. Biol. Chem.* **2002**, *277*, 559–565. [[CrossRef](#)] [[PubMed](#)]
33. Wang, L.; Eggenberger, A.; Hill, J.; Bogdanove, A.J. *Pseudomonas syringae* effector avrB confers soybean cultivar-specific avirulence on Soybean mosaic virus adapted for transgene expression but effector avrPto does not. *Mol. Plant Microbe Interact.* **2006**, *19*, 304–312. [[CrossRef](#)] [[PubMed](#)]
34. Meng, X.; Zhang, S. MAPK cascades in plant disease resistance signaling. *Annu. Rev. Phytopathol.* **2013**, *51*, 245–266. [[CrossRef](#)]
35. Zhao, C.; Nie, H.; Shen, Q.; Zhang, S.; Lukowitz, W.; Tang, D. EDR1 physically interacts with MKK4/MKK5 and negatively regulates a MAP kinase cascade to modulate plant innate immunity. *PLoS Genet.* **2014**, *10*, e1004389. [[CrossRef](#)]
36. Ma, C.; Liu, Y.; Bai, B.; Han, Z.; Tang, J.; Zhang, H.; Yaghmaiean, H.; Zhang, Y.; Chai, J. Structural basis for BIR1-mediated negative regulation of plant immunity. *Cell Res.* **2017**, *27*, 1521–1524. [[CrossRef](#)]
37. Wierzbica, M.P.; Tax, F.E. An allelic series of bak1 mutations differentially alter bir1 cell death, immune response, growth, and root development phenotypes in *Arabidopsis thaliana*. *Genetics* **2016**, *202*, 689–702. [[CrossRef](#)]
38. Guzmán-Benito, I.; Donaire, L.; Amorim-Silva, V.; Vallarino, J.G.; Esteban, A.; Wierzbicki, A.T.; Ruiz-Ferrer, V.; Llave, C. The immune repressor BIR1 contributes to antiviral defense and undergoes transcriptional and post-transcriptional regulation during viral infections. *New Phytol.* **2019**, *224*, 421–438. [[CrossRef](#)]
39. Schmutz, J.; Cannon, S.B.; Schlueter, J.; Ma, J.; Mitros, T.; Nelson, W.; Hyten, D.L.; Song, Q.; Thelen, J.J.; Cheng, J. Genome sequence of the palaeopolyploid soybean. *Nature* **2010**, *463*, 178–183. [[CrossRef](#)]
40. Zhang, Z.; Wu, Y.; Gao, M.; Zhang, J.; Kong, Q.; Liu, Y.; Ba, H.; Zhou, J.; Zhang, Y. Disruption of PAMP-induced MAP kinase cascade by a *Pseudomonas syringae* effector activates plant immunity mediated by the NB-LRR protein SUMM2. *Cell Host Microbe* **2012**, *11*, 253–263. [[CrossRef](#)]
41. Kong, Q.; Qu, N.; Gao, M.; Zhang, Z.; Ding, X.; Yang, F.; Li, Y.; Dong, O.X.; Chen, S.; Li, X.; et al. The MEKK1-MKK1/MKK2-MPK4 kinase cascade negatively regulates immunity mediated by a mitogen-activated protein kinase kinase kinase in Arabidopsis. *Plant Cell* **2012**, *24*, 2225–2236. [[CrossRef](#)] [[PubMed](#)]
42. Takagi, M.; Hamano, K.; Takagi, H.; Morimoto, T.; Akimitsu, K.; Terauchi, R.; Shirasu, K.; Ichimura, K. Disruption of the MAMP-Induced MEKK1-MKK1/MKK2-MPK4 Pathway Activates the TNL Immune Receptor SMN1/RPS6. *Plant Cell Physiol.* **2019**, *60*, 778–787. [[CrossRef](#)] [[PubMed](#)]
43. Whitham, S.; Dinesh-Kumar, S.P.; Choi, D.; Hehl, R.; Corr, C.; Baker, B. The product of the tobacco mosaic virus resistance gene N: Similarity to toll and the interleukin-1 receptor. *Cell* **1994**, *78*, 1101–1115. [[CrossRef](#)]
44. Yang, S.; Hua, J. A haplotype-specific Resistance gene regulated by BONZAI1 mediates temperature-dependent growth control in Arabidopsis. *Plant Cell* **2004**, *16*, 1060–1071. [[CrossRef](#)]
45. Wiermer, M.; Feys, B.J.; Parker, J.E. Plant immunity: EDS1 regulatory node. *Curr. Opin. Plant Biol.* **2005**, *8*, 383–389. [[CrossRef](#)] [[PubMed](#)]
46. Yuan, M.; Jiang, Z.; Bi, G.; Nomura, K.; Liu, M.; Wang, Y.; Cai, B.; Zhou, J.M.; He, S.Y.; Xin, X.F. Pattern-recognition receptors are required for NLR-mediated plant immunity. *Nature* **2021**, *592*, 105–109. [[CrossRef](#)]
47. Ngou, B.P.M.; Ahn, H.K.; Ding, P.; Jones, J.D.G. Mutual potentiation of plant immunity by cell-surface and intracellular receptors. *Nature* **2021**, *592*, 110–115. [[CrossRef](#)]
48. Zhang, C.; Yang, C.; Whitham, S.A.; Hill, J.H. Development and use of an efficient DNA-based viral gene silencing vector for soybean. *Mol. Plant Microbe Interact.* **2009**, *22*, 123–131. [[CrossRef](#)]
49. Zhang, C.; Bradshaw, J.D.; Whitham, S.A.; Hill, J.H. The development of an efficient multipurpose bean pod mottle virus viral vector set for foreign gene expression and RNA silencing. *Plant Physiol.* **2010**, *153*, 52–65. [[CrossRef](#)]
50. Liu, J.Z.; Blancaflor, E.B.; Nelson, R.S. The tobacco mosaic virus 126-kilodalton protein, a constituent of the virus replication complex, alone or within the complex aligns with and traffics along microfilaments. *Plant Physiol.* **2005**, *138*, 1853–1865. [[CrossRef](#)]
51. Zhang, K.; Halitschke, R.; Yin, C.; Liu, C.J.; Gan, S.S. Salicylic acid 3-hydroxylase regulates Arabidopsis leaf longevity by mediating salicylic acid catabolism. *Proc. Natl. Acad. Sci. USA* **2013**, *110*, 14807–14812. [[CrossRef](#)] [[PubMed](#)]

52. Jefferson, R.A.; Kavanagh, T.A.; Bevan, M.W. GUS fusions: Beta-glucuronidase as a sensitive and versatile gene fusion marker in higher plants. *EMBO J.* **1987**, *6*, 3901–3907. [[CrossRef](#)] [[PubMed](#)]
53. Goodin, M.; Dietzgen, R.G.; Schichnes, D.; Ruzin, S.; Jackson, A.O. pGD vectors: Versatile tools for the expression of green and red fluorescent protein fusions in Agroinfiltrated plant leaves. *Plant J.* **2002**, *31*, 375–383. [[CrossRef](#)] [[PubMed](#)]